

Recoupling the non-secular part of nuclear spin-spin interaction in solids

Chahan M. Kropf* and Boris V. Fine†

Institute for Theoretical Physics, University of Heidelberg, Philosophenweg 19, 69120 Heidelberg, Germany
(Dated: February 6, 2012)

NMR spin-spin relaxation in solids in strong magnetic fields is normally described only with the help of the secular part of the full spin-spin interaction Hamiltonian. This approximation is associated with the averaging of the spin-spin interaction over the fast motion of spins under the combined action of the static and the radio-frequency (rf) fields. Here we report a set of conditions (recoupling resonances) when the averaging over the above fast motion preserves some of the non-secular terms entering the full interaction Hamiltonian. These conditions relate the value of the static magnetic field with the frequency and the amplitude of the rf field. When the above conditions are satisfied, the effective recoupled spin-spin interaction Hamiltonian has an unconventional form with tunable parameters. These tunable Hamiltonian offers interesting possibilities to manipulate nuclear spins in solids and can shed new light on the fundamental properties of the nuclear spin-spin relaxation phenomenon.

PACS numbers: 76.60.-k, 76.60.Es

I. INTRODUCTION

The experimental technique of nuclear magnetic resonance (NMR) has long established itself as a versatile tool for microscopic investigations of matter. One major source of microscopic information in NMR is the spin-spin relaxation. In solids, the description of NMR spin-spin relaxation requires averaging the full Hamiltonian of nuclear spin-spin interaction over the fast spin rotations induced by strong external magnetic fields. The present paper predicts theoretically a set of resonant conditions for solid-state NMR experiments leading to an unconventional form of the averaged interaction Hamiltonians.

We consider nuclear spin-spin interactions in the presence of a static magnetic field and a continuously applied *rotating* radio-frequency (rf) field in the regime, when the two fields have comparable values, while both of them are still much larger than the local fields with which nuclear spins affect each other. Such a setting is realizable experimentally. However, it implies the use of smaller-than-typical static fields and, therefore, a certain sacrifice in terms of the signal intensity. In a typical NMR experiment, the rf-field may be large in comparison with the local fields, but it is still much smaller than the static field. This “typical” setting for strong continuously applied rf fields was originally considered by Redfield¹ and subsequently discussed in NMR textbooks^{2,3}. In such a case, the averaged interaction Hamiltonian is obtained from the full Hamiltonian with the help of a two-step truncation procedure¹. The first step is to eliminate all interaction terms that do not commute with the Zeeman Hamiltonian for the static magnetic field⁴. The second step is to make the transformation into the rotating reference frame where the rf field appears static, and then further truncate the interaction Hamiltonian by eliminating all the terms that do not commute with the Zeeman Hamiltonian for the effective magnetic field in the rotating frame.

When the static and the rf fields are comparable to

each other, the validity of the above two-step truncation becomes questionable, because the spin motions caused by both fields fall on the same timescale. The full interaction Hamiltonian then needs to be averaged over the above two motions simultaneously rather than in two independent steps. In this paper, we show that, in the case of a purely rotating rf field (as opposed to the case of a linearly-polarized rf field), such a single step averaging can be done rigorously without requiring the rf field to be smaller than the static field. We find that such a single-step procedure generically reproduces the results of Redfield’s two-step truncation, but the reason for this agreement lies not in the perturbation theory but in the ergodic character of the single-spin dynamics driven by the static and the rf fields. We also find that in certain special cases, which we call “recoupling resonances”, the averaged spin-spin interaction Hamiltonian includes other terms in addition to the outcome of Redfield’s truncation procedure. In the case of single spin species, the recoupling resonances appear when the rf field frequency is matched with certain multiples or simple fractions of the Larmor frequency corresponding to the effective magnetic field in the rotating reference frame. In the case of two different spin species, the sums and the differences of the two effective Larmor frequencies also appear in some of the recoupling resonance conditions. The time-averaged interaction Hamiltonians associated with the above recoupling resonances are non-secular, in the sense that they do not conserve the total Zeeman energy associated with the external fields in either the laboratory or the rotating reference frame. These Hamiltonians may have a range of applications, such as, e.g., nuclear cross-polarization, or molecular structure determination.

It is worth noting that the term “recoupling” is extensively used^{5–8} in the context of the magic angle spinning (MAS) technique of NMR, where it implies the recovery of a part of the standard truncated Hamiltonian, after that Hamiltonian was suppressed by the spinning of the sample. The MAS recoupling schemes match the fre-

quency of the spin nutation⁵ or the frequency of the rf pulses^{6–8} with the multiples of the sample spinning frequency. In the present paper, the term “recoupling” is used at a more basic level: it implies the recovery of a part of the *full* spin-spin interaction Hamiltonian lost in the standard truncation procedure. The recoupling resonances described below have nothing to do with sample spinning. However, they are best observable and, probably, most useful in combination with MAS.

In a broader context, our results could have been obtained in the framework of the averaged Hamiltonian theory⁹, but to the best of our knowledge it has never been attempted, perhaps because of the non-perturbative character of the problem. The role of the non-secular terms was, however, discussed in the context of the phenomenon of nuclear spin superradiance^{10,11}.

The rest of this paper is organized as follows. We give the general formulation of the problem in Section II, introduce our single-step truncation procedure in Section III, present the results of this truncation with the identification of the recoupling resonances in Section IV, and then discuss a possible experimental test and possible applications of the recoupling resonances in Section V.

II. GENERAL FORMULATION

We consider a lattice of nuclear spins in a static magnetic field pointing along the z -axis, $\mathbf{H}_0 \equiv (0, 0, H_0)$, irradiated by a rf field rotating in the x - y plane with frequency ω , $\mathbf{H}_1(t) \equiv (H_1 \cos \omega t, H_1 \sin \omega t, 0)$. We limit ourselves to the case of the magnetic dipole spin-spin interaction, which is, typically, dominant in solids. The full Hamiltonian^{2,3} is

$$\mathcal{H} = \mathcal{H}_z + \mathcal{H}_{\text{rf}} + \mathcal{H}_D \quad (1)$$

where

$$\mathcal{H}_z = -H_0 \sum_i \gamma_i I_{iz}, \quad (2)$$

$$\mathcal{H}_{\text{rf}} = -\mathbf{H}_1(t) \cdot \sum_i \gamma_i \mathbf{I}_i, \quad (3)$$

and

$$\mathcal{H}_D = \sum_{i < j} J_{ij} [\mathbf{I}_i \cdot \mathbf{I}_j - \frac{3 \cdot (\mathbf{I}_i \cdot \mathbf{r}_{ij})(\mathbf{I}_j \cdot \mathbf{r}_{ij})}{r_{ij}^2}]. \quad (4)$$

Here $J_{ij} = \frac{\gamma_i \gamma_j \hbar^2}{r_{ij}^3}$ are the coupling constants, $\mathbf{I}_i \equiv (I_{ix}, I_{iy}, I_{iz})$ are the operators of the nuclear spin of the i th lattice site, γ_i is the gyromagnetic ratio of that spin, $\mathbf{r}_{ij} \equiv (r_{ij,x}, r_{ij,y}, r_{ij,z})$ are the displacement vectors between two lattice sites i and j , and N is the number

of spins. The characteristic time of a single spin motion induced by the Hamiltonian \mathcal{H}_D can be estimated as $T_2 = \hbar \left(\sum_j J_{ij}^2 \right)^{-1/2}$. The variable T_2 is also to be referred to as the transverse relaxation time. The timescale of nuclear spin relaxation due to the coupling to electrons or phonons is to be denoted as T_1 (longitudinal relaxation time). We further introduce the Larmor frequencies $\Omega_{0i} = \gamma_i H_0$ and the nutation frequencies $\omega_{1i} = \gamma_i H_1$. In the following, we drop lattice index i in the gyromagnetic ratio and use the notations $\gamma \equiv \gamma_i$, $\Omega_0 = \gamma H_0$, $\omega_1 = \gamma H_1$, etc., when not dealing with the interactions of non-equivalent (unlike) spins explicitly.

This paper is limited to the regime $\Omega_0, \omega_1 \gg 1/T_2 \gg 1/T_1$. The first of these inequalities implies the separation of the timescales between the fast motion due to the external fields and the slow motion due to the spin-spin interaction. The second inequality allows us to consider the nuclear spins as isolated from the environment. As mentioned in the introduction, the theoretical analysis in the literature^{1–3} was limited so far by the additional inequality $H_1 \ll H_0$ (i.e. $\omega_1 \ll \Omega_0$). Our main focus is on the regime $H_1 \sim H_0$. However, also, for a range of situations satisfying the inequality $H_1 \ll H_0$, the recoupling resonances obtained below will imply important observable effects.

III. TRUNCATION PROCEDURE

We calculate the effective spin-spin interaction Hamiltonian by averaging the full interaction Hamiltonian \mathcal{H}_D over the fast spin motion induced by the terms $\mathcal{H}_z + \mathcal{H}_{\text{rf}}$. In the Heisenberg representation, this fast motion is described by the following equation for each of the spins :

$$\frac{d\mathbf{I}_i}{dt} = \mathbf{I}_i \times \gamma \mathbf{H}(t), \quad (5)$$

where $\mathbf{H}(t) = \mathbf{H}_0 + \mathbf{H}_1(t)$. The above equation is linear in terms of spin operators (I_{ix}, I_{iy}, I_{iz}) , and, therefore, its predictions are essentially the same as those for the classical spins, in which case (I_{ix}, I_{iy}, I_{iz}) would be simply three numbers. Despite the linearity of Eq.(5), it is not solvable analytically either classically or quantum mechanically for an arbitrary time-dependent $\mathbf{H}(t)$. However, for the specific time dependence considered in this work, the solution is facilitated by the transformation from the laboratory reference frame into the reference frame rotating around the z -axis with frequency ω . The equations of motion in the rotating frame have the same form as Eq.(5), but with time-independent effective magnetic field $\mathbf{H}_e = (H_1, 0, H_0 + \omega/\gamma)$. (The x -axis in the rotating frame coincides with the direction of the rf field.) The corresponding Larmor frequency is

$$\Omega_e = \gamma H_e = \text{sign}(\gamma) \sqrt{\omega_1^2 + (\Omega_0 + \omega)^2}. \quad (6)$$

Thus, the motion of a spin in the laboratory frame can be characterized as the Larmor precession with frequency Ω_e around the direction of \mathbf{H}_e , which itself rotates with frequency ω around the z -axis.

Our formal procedure for averaging \mathcal{H}_D consists of the transformation into the reference frame that follows the fast spin rotation induced by Eq.(5). In that reference frame, each spin would be motionless, if the full Hamiltonian included only $\mathcal{H}_z + \mathcal{H}_{\text{rf}}$. Such a transformation is time-dependent. As a result, the Hamiltonian \mathcal{H}_D expressed in the new spin coordinates acquires some quickly oscillating interaction coefficients, which we then average out.

The above procedure may, at first sight, appear equivalent to the one introduced by Redfield¹⁻³. The difference, however, is that Redfield did not define the entire transformation and then average the resulting Hamiltonian over time but rather used the Zeeman-energy-conservation criterion of Van Vleck⁴ to average separately the Hamiltonians obtained at the intermediate steps of this transformation. Such an independent averaging of the intermediate Hamiltonians is justifiable by the perturbation theory arguments¹ only when $\Omega_0 \gg \omega_1$. It is shown below, that in the case of $\Omega_0 \sim \omega_1$, the spin motions associated with the intermediate transformation steps may be correlated, and thus the averaging over them cannot be done independently.

The overall transformation into the reference frame that follows the motion induced by Eq.(5) can be decomposed into three simple transformations visualized in Fig.1. The first transformation is from the laboratory frame to the reference frame rotating with the rf field:

$$U_\omega = \begin{pmatrix} \cos(\omega t) & \sin(\omega t) & 0 \\ -\sin(\omega t) & \cos(\omega t) & 0 \\ 0 & 0 & 1 \end{pmatrix}. \quad (7)$$

The second transformation is from the rotating to the “tilted-rotating” reference frame, where the z -axis coincides with the direction of \mathbf{H}_e :

$$U_\alpha = \begin{pmatrix} \cos \alpha & 0 & -\sin \alpha \\ 0 & 1 & 0 \\ \sin \alpha & 0 & \cos \alpha \end{pmatrix}, \quad (8)$$

with

$$\alpha = \text{arccot} \left[\frac{\Omega_0 + \omega}{\omega_1} \right], \quad (9)$$

admitting values in the range $[0, \pi]$.

Finally, the third transformation is into the “double-rotating” reference frame precessing around \mathbf{H}_e with frequency $-\Omega_e$:

$$U_{\Omega_e} = \begin{pmatrix} \cos(\Omega_e t) & -\sin(\Omega_e t) & 0 \\ \sin(\Omega_e t) & \cos(\Omega_e t) & 0 \\ 0 & 0 & 1 \end{pmatrix}. \quad (10)$$

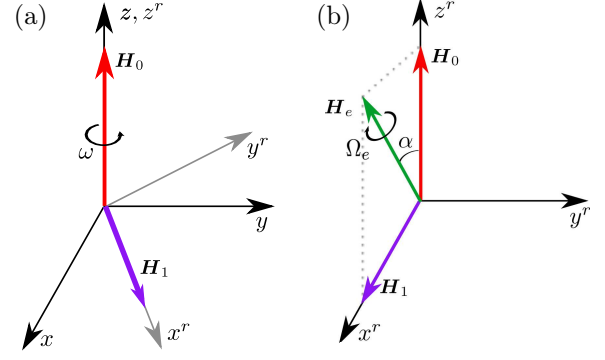


Figure 1: (a) Illustration of the transformation from the laboratory reference frame (x, y, z) to the rotating reference frame (x^r, y^r, z^r) — Eq.(7). (b) Illustration for the transformation from the rotating reference frame (x^r, y^r, z^r) to the tilted-rotating and then double-rotating reference frames — Eqs.(8,10).

The effective magnetic field in this reference frame is equal to zero. The explicit implementation of transformation (10) before performing the time-averaging of \mathcal{H}_D formally discriminates our treatment from that of Redfield¹⁻³.

We denote the axes in the double-rotated reference frame as $\{x', y', z'\}$, and the corresponding spin projections as $\mathbf{I}'_i \equiv (I'_{ix}, I'_{iy}, I'_{iz})$. The spin coordinates in the laboratory reference frame can now be expressed as

$$\mathbf{I}_i = U_\omega^{-1} U_\alpha^{-1} U_{\Omega_e}^{-1} \mathbf{I}'_i. \quad (11)$$

The substitution of Eq.(11) into Eq.(4) allows us to reexpress the interaction Hamiltonian \mathcal{H}_D in terms of \mathbf{I}'_i and then average the interaction coefficients in the resulting expression.

The full time-dependent form of \mathcal{H}_D in the double-rotated reference frame is rather long. It can be found in Ref.¹² together with the implementation of the time-averaging procedure. Below we exemplify this procedure by one typical term and then, in the next section, present only the resulting time-averaged expressions for \mathcal{H}_D .

The term we have chosen as an example, originates from the calculation for equivalent (like) spin species discussed in the next section. It has form

$$a_{ij}(t) c(\mathbf{r}_{ij}) I'_{ix} I'_{jx}, \quad (12)$$

where $c(\mathbf{r}_{ij})$ is some function of the relative displacement between the two nuclei, and

$$a_{ij}(t) = \cos^2(\omega t) \cos^2(\Omega_e t). \quad (13)$$

The time-averaged value of the above coefficient is calculated as follows

$$\langle a_{ij} \rangle = \lim_{\tau \rightarrow \infty} \frac{1}{2\tau} \int_{-\tau}^{\tau} a_{ij}(t) dt = \begin{cases} \frac{1}{4} & \text{if } \omega \neq \pm \Omega_e, \\ \frac{3}{8} & \text{if } \omega = \pm \Omega_e. \end{cases} \quad (14)$$

In the above case, $\langle a_{ij} \rangle = \frac{1}{4}$ is what one obtains by the standard two-step truncation procedure outlined in the introduction, while, in the case of $\omega = \pm\Omega_e$, there is an extra contribution associated with the fact that $\langle \cos^2(\omega t) \cos^2(\Omega_e t) \rangle \neq \langle \cos^2(\omega t) \rangle \langle \cos^2(\Omega_e t) \rangle$.

The question then arises, what happens, if, in an experiment, the actual values of H_0 , H_1 and ω are such that one of the recoupling resonance conditions is satisfied approximately but not exactly. In such a case, the Hamiltonian-averaging procedure needs to be modified. Below, we illustrate this modification for the resonant condition $\omega = -\frac{1}{2}\Omega_e$ but the expression for the resulting correction to the averaged Hamiltonian is applicable to all other recoupling resonances.

In the chosen example, the mismatch of the resonant condition can be parameterized with the help of variable $\Delta\Omega_e$ defined by equation $\omega = -\frac{1}{2}(\Omega_e + \Delta\Omega_e)$. Now we modify the last step of the transformation to the double-rotated reference frame [Eq.(10)] by changing the value of the rotation frequency from Ω_e given by Eq.(6) to $\Omega_e + \Delta\Omega_e$. In the modified double-rotated reference frame, the averaged interaction Hamiltonian obtained in Section IV A for the recoupling resonance $\omega = -\frac{1}{2}\Omega_e$ will be exactly valid, but, in addition, since $\Omega_e + \Delta\Omega_e$ is different from Ω_e , the effective magnetic field will be different from zero, which then gives rise to the following additional term:

$$\Delta\mathcal{H} = \Delta\Omega_e \sum_i I'_{iz}. \quad (15)$$

When $\Delta\Omega_e \gg 1/T_2$, such a term suppresses the effect of the resonant non-secular terms given in the next section. This is, of course, expected for a significant departure from the recoupling resonance conditions. When $\Delta\Omega_e \sim 1/T_2$, the above term still suppresses the effect of the non-secular terms but only partially, and this partial suppression is of the same order of magnitude as the suppression caused by the secular interaction terms (to be explained in Section IV A). In such a case, the term (15) should simply be included in the averaged Hamiltonian together with the secular terms and the resonant non-secular terms.

The above considerations imply, that, in a generic case, when the strength of the secular terms can be estimated as \hbar/T_2 , the recoupling resonance conditions cannot be resolved experimentally with accuracy much better than $\pm 1/T_2$. However, if the secular terms are suppressed by other means, then the experimental resolution will be limited by the strength of the recoupled terms themselves. Thus, if the strength of the recoupled terms is much smaller than \hbar/T_2 , then the recoupling resonances can be resolvable with proportionally better accuracy.

Let us now think about the averaging procedure in terms of classical spin trajectories. The typical situation corresponds to an irrational value of the ratio ω/Ω_e . In this case, the trajectory of a classical spin that follows Eq.(5) is open and ergodic on the spin sphere, as

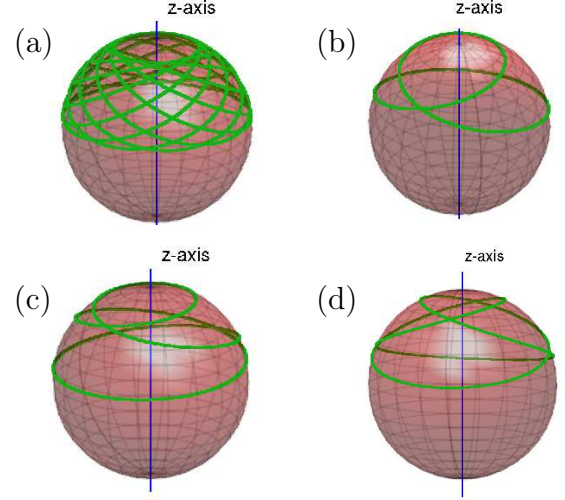


Figure 2: Examples of trajectories of a single classical spin under the combined action of the static and the rf magnetic fields: (a) general case, open ergodic trajectory; (b) $\omega = -\Omega_e$, closed trajectory; (c) $\omega = -2\Omega_e$, closed trajectory; (d) $\omega = \frac{1}{2}\Omega_e$, closed trajectory.

illustrated in Fig. 2(a). Averaging over such trajectories leads to the standard two-step truncation result. If ω/Ω_e is a rational number, then the individual spin trajectories become closed, and one can suspect that the averaging result is different from the irrational case. In reality, however, almost all rational values of ω/Ω_e lead to the same averaging results as the irrational values. In the case of like spins, the only exceptions are $\omega/\Omega_e = \{\pm 1/2, -1, -2\}$ —see Figs. 2(b-d). The fact that no other rational numbers appear in this set is related to the fact that the interaction Hamiltonian \mathcal{H}_D is of the second order in terms of spin variables. If higher order spin couplings were involved, e.g. of the form $I_{ix}I_{jx}I_{ky}$, then other ratios with absolute values such as $1/3$ or 3 may also appear in the above set.

IV. RESULTS

In this section, we present the time-averaged Hamiltonians separately for the couplings of “like” spins (subsection IV A) and “unlike” spins (subsection IV B). Like spins have the same gyromagnetic ratios and hence the same Larmor frequencies. Unlike spins have different gyromagnetic ratios and different Larmor frequencies. The Hamiltonians referring to the above two cases are marked by superscripts l and u , respectively. The details of the calculations can be found in Ref.¹².

A. Like spins

Away from the recoupling resonances, our averaging procedure reproduces the standard truncated Hamiltonian for like spins³:

$$\mathcal{H}_{D0}^l = \sum_{i < j}^N J_{ij} \frac{1}{2} (3 \cos^2 \alpha - 1) \left(1 - \frac{3r_{ij,z}^2}{r_{ij}^2} \right) \times \left[I'_{iz} I'_{jz} - \frac{1}{2} (I'_{ix} I'_{jx} + I'_{iy} I'_{jy}) \right], \quad (16)$$

where α is given by Eq.(9).

As already mentioned in Section III, the averaged Hamiltonian contains additional coupling terms in the case of recoupling resonances associated with ratios $\omega/\Omega_e = \{\pm 1/2, -1, -2\}$. According to Eq.(6), these ratios translate into the following expressions for ω in terms of Ω_0 and ω_1 :

$$\omega = -\Omega_e : \quad \omega = -\frac{\omega_1^2 + \Omega_0^2}{2\Omega_0}; \quad (17)$$

$$\omega = -2\Omega_e : \quad \omega = \frac{-4\Omega_0 \pm 2\sqrt{\Omega_0^2 - 3\omega_1^2}}{3}; \quad (18)$$

$$\omega = \pm \frac{1}{2}\Omega_e : \quad \omega = \frac{\Omega_0 \pm \sqrt{4\Omega_0^2 + 3\omega_1^2}}{3}. \quad (19)$$

The upper (lower) sign before the square root in Eq.(19) corresponds to the upper (lower) sign of the resonant condition $\omega = \pm \frac{1}{2}\Omega_e$. In the case of Eq.(18) both signs before the square root are realizable for the same condition $\omega = -2\Omega_e$ as long as $|\Omega_0| \geq \sqrt{3}|\omega_1|$. When the value of ω following from Eq.(17),(18) or (19) is negative, this indicates that frequency vector $\boldsymbol{\omega}$ is anti-parallel to \mathbf{H}_0 . The resonance conditions $\omega = \Omega_e$ and $\omega = 2\Omega_e$ are absent in the above list, because, after the substitution of Ω_e given by Eq.(6) they give no real-valued solutions for ω .

Now we list the corresponding averaged Hamiltonians:

$$\omega = -\Omega_e : \quad \mathcal{H}_{D1}^l = \mathcal{H}_{D0}^l + \sum_{i < j}^N J_{ij} \left\{ \frac{3}{8} (\cos \alpha - 1)^2 \left[\frac{r_{ij,y}^2 - r_{ij,x}^2}{r_{ij}^2} (I'_{ix} I'_{jx} - I'_{iy} I'_{jy}) + \frac{2 r_{ij,x} r_{ij,y}}{r_{ij}^2} (I'_{ix} I'_{jy} + I'_{iy} I'_{jx}) \right] \right. \\ \left. + \frac{3}{2} (\cos 2\alpha - \cos \alpha) \left[-\frac{r_{ij,x} r_{ij,z}}{r_{ij}^2} (I'_{ix} I'_{jz} + I'_{iz} I'_{jx}) + \frac{r_{ij,y} r_{ij,z}}{r_{ij}^2} (I'_{iy} I'_{jz} + I'_{iz} I'_{jy}) \right] \right\}; \quad (20)$$

$$\omega = -2\Omega_e : \quad \mathcal{H}_{D2}^l = \mathcal{H}_{D0}^l + \sum_{i < j}^N J_{ij} \frac{3}{4} [\sin 2\alpha - 2 \sin \alpha] \left[\frac{r_{ij,x} r_{ij,z}}{r_{ij}^2} (I'_{ix} I'_{jx} - I'_{iy} I'_{jy}) - \frac{r_{ij,y} r_{ij,z}}{r_{ij}^2} (I'_{ix} I'_{jy} + I'_{iy} I'_{jx}) \right]; \quad (21)$$

$$\omega = \pm \frac{1}{2}\Omega_e : \quad \mathcal{H}_{D3}^l = \mathcal{H}_{D0}^l + \sum_{i < j}^N J_{ij} \frac{3}{8} [\sin 2\alpha \pm 2 \sin \alpha] \left[\frac{r_{ij,y}^2 - r_{ij,x}^2}{r_{ij}^2} (I'_{ix} I'_{jz} + I'_{iz} I'_{jx}) \mp \frac{2 r_{ij,x} r_{ij,y}}{r_{ij}^2} (I'_{iy} I'_{jz} + I'_{iz} I'_{jy}) \right]. \quad (22)$$

The upper (lower) sign of the resonance condition of Eq.(22) corresponds to the upper (lower) sign in the expression for \mathcal{H}_{D3}^l .

We note that the standard truncated Hamiltonian \mathcal{H}_{D0}^l conserves the z' -projection of the total spin polarization $\sum_i I'_{iz}$ in the double-rotating reference frame. This total spin component still relaxes on the time scale of the order of T_1 because of the interaction with electronic spins or phonons. We call this “normal longitudinal relaxation.” In contrast, the recoupled terms appearing in Eqs.(20-22) do not conserve $\sum_i I'_{iz}$, which means that all three projections of the total spin polarization decay to

zero in both the double-rotating and the laboratory reference frames on a time scale, which is, in general, much faster than T_1 . We call this “anomalous longitudinal relaxation.”

The recoupled terms in Eqs.(20-22) are comparable with \mathcal{H}_{D0}^l , when $H_1 \sim H_0$. In such a case, the time scale of the anomalous longitudinal relaxation is expected to be of the order of T_2 , which is clearly much faster than T_1 . Therefore, the recoupling resonances should be readily identifiable in an experiment of the type proposed in Section V A.

In the case of $H_1 \ll H_0$, the recoupled terms can still

induce the anomalously fast longitudinal relaxation, but this case requires a more detailed discussion. We first note that all recoupled terms in Eqs.(20-22) are equal to zero, when $\alpha = 0$, which, according to Eq.(9), corresponds to $H_1 = 0$. When $H_1 \ll H_0$, the recoupled terms are much smaller than the terms in \mathcal{H}_{D0}^l , in agreement with the standard truncation result of Redfield¹⁻³. The values of the α -dependent prefactors of the recoupled terms in the Hamiltonians (20-22) are plotted as functions of H_1/H_0 in Fig.3 for $H_1/H_0 \leq 0.5$. The strongest of these terms are of the order of H_1/H_0 . They correspond to the resonances $\omega \approx \Omega_0$ and $\omega \approx -2\Omega_0$ obtained, respectively, from Eq.(18) with plus sign and Eq.(19) with minus sign in the limit $H_1/H_0 \rightarrow 0$. (In our sign convention, the usual single-spin NMR resonance is located at $\omega \approx -\Omega_0$.)

In general, the recoupled terms linear in H_1/H_0 should induce a longitudinal relaxation on the time scale of the order of $T_2(H_0/H_1)^2$, which can still be much shorter than T_1 and thus represent a clear indication of a recoupling resonance. The above estimate is of the second order in terms of H_0/H_1 , because the first-order effect of the recoupled terms should be averaged out by the spin motions due to the much stronger secular terms. In view of this consideration, the observability of the recoupling resonances can be significantly improved by suppressing the secular Hamiltonian \mathcal{H}_{D0}^l . If this is done, the timescale of the longitudinal relaxation induced by the recoupled terms can be estimated as $T_2(H_0/H_1)$, i.e. it becomes much faster.

The suppression of \mathcal{H}_{D0}^l makes the observable effects of the recoupling resonances more dramatic not only in the limit of $H_1 \ll H_0$, but also in the general case of $H_1 \sim H_0$. It can be realized, for example, as follows.

A given recoupling resonance imposes a constraint on the three parameters H_0 , H_1 and ω , which leaves a freedom to impose one additional relationship. This freedom can be used to impose the magic angle condition $1 - 3\cos^2\alpha = 0$. However, this condition together with any of the like-spin recoupling resonances fixes the ratio H_1/H_0 to be of the order of 1, which means that it cannot be used if the experiment is limited to the regime $H_1 \ll H_0$.

Another resource for suppressing \mathcal{H}_{D0}^l is to exploit the spatially dependent factor $1 - \frac{3r_{ij,z}^2}{r_{ij}^2}$. For example, if the recoupling resonances are to be investigated in CaF_2 , where ^{19}F nuclei form a simple cubic lattice, it is better to use the static field along the [111] direction of that lattice. In such a case, $1 - \frac{3r_{ij,z}^2}{r_{ij}^2} = 0$ for all six nearest neighbors of each spin, i.e. the secular interaction with these neighbors is suppressed, while the recoupled terms remain large.

Of course, the most effective way to suppress the secular interactions for all pairs of interacting spins is to use the MAS technique³. This technique completely averages out all factors $1 - \frac{3r_{ij,z}^2}{r_{ij}^2}$, when $\cos^2\Theta = 1/3$, where

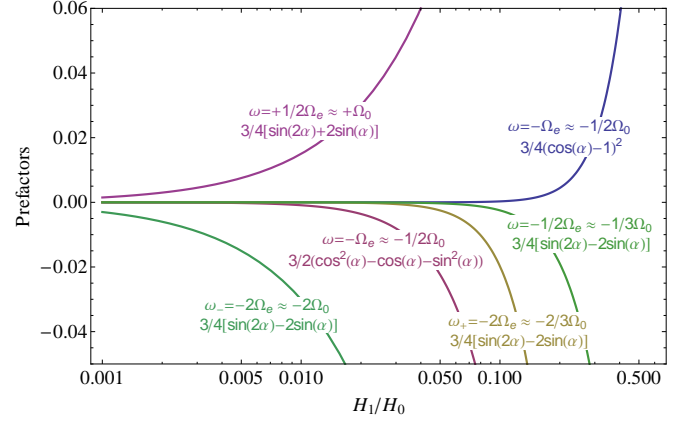


Figure 3: (Color online) Plots of the α -dependent prefactors of the recoupled terms in the like-spin Hamiltonians (20-22) as functions of the ratio H_1/H_0 for $H_1 < 0.5H_0$. The legend for each line indicates the corresponding resonant condition and the α -dependence of the prefactor being plotted. Each resonant condition is given both in its exact form (17-19) and in the approximate form for the case $H_1 \ll H_0$. The conditions $\omega_+ = -2\Omega_e$ and $\omega_- = -2\Omega_e$ correspond to the recoupling resonances (18) with signs (+) or (-), respectively.

Θ is the “magic” angle between the spinning axis and the static magnetic field. Spinning at the magic angle, however, does not average out completely the factors $r_{ij,y}^2 - r_{ij,x}^2$, $r_{ij,x}r_{ij,y}$, or $r_{ij,x}r_{ij,z}$ that enter the recoupled Hamiltonians.

B. Unlike spins

In this subsection, we consider coupling between two unlike spin species. We will use lattice index i to label one of these species and index j to label the other. We reintroduce the labeling of gyromagnetic ratios γ_i and γ_j , and the corresponding Larmor frequencies $\Omega_{0i} = \gamma_i H_0$ and $\Omega_{0j} = \gamma_j H_0$. The two spin species are now to be described in two different double-rotated reference frames. The effective Larmor frequencies Ω_{ei} , Ω_{ej} and the corresponding tilting angles α_i , α_j are then defined by adding the indices i or j to variable Ω_e , Ω_0 , ω_1 and α in Eqs.(6) and (9).

As in the case of like spins, our averaging procedure for unlike spins recovers the standard truncated Hamiltonian³ away from the recoupling resonances:

$$\mathcal{H}_{D0}^u = \sum_{\langle i,j \rangle} J_{ij} \frac{1}{2} [3 \cos \alpha_i \cos \alpha_j - \cos(\alpha_i - \alpha_j)] \times \left(1 - \frac{3r_{ij,z}^2}{r_{ij}^2} \right) I'_{iz} I'_{jz}, \quad (23)$$

where the sum $\sum_{\langle i,j \rangle}$ includes all pairs of unlike spins.

It should be mentioned here, that, in the very special

case of $\gamma_i = -\gamma_j$ and $\omega = 0$, the secular Hamiltonian \mathcal{H}_{D0}^u should also include the so-called “double-flip” terms $I'_{i+}I'_{j+}$ and $I'_{i-}I'_{j-}$, where $I'_{i\pm} = I'_{ix} \pm I'_{iy}$, etc. These terms are preserved by the averaging, because their counterparts $I_{i+}I_{j+}$ and $I_{i-}I_{j-}$ in the original full Hamiltonian (1) now conserve the Zeeman energy. This case can be mapped onto a somewhat unusual problem of like spins by changing the sign of all y- and z- spin projections for one of the two spin species, e.g. $I_{jy} \rightarrow -I_{jy}$ and $I_{jz} \rightarrow -I_{jz}$. However, when $\omega \neq 0$, the two spin species in the transformed problem will experience rf-fields rotating in the opposite directions, which means that the transformed problem is not equivalent to the problem of like spins in a single rotating field.

Another special case is $\gamma_j \rightarrow 0$. It implies that the terms of the type $I_{iz}I_{j\pm}$ in the full Hamiltonian (1) become secular, and, as a result, terms $I'_{iz}I'_{j\pm}$ may appear in \mathcal{H}_{D0}^u . Such a limit is not realizable physically in the case of magnetic dipole interaction, because $\gamma_j = 0$ simultaneously suppresses the interaction itself.

The above special cases should be kept in mind in the analysis of the parameter dependence of the recoupling resonances.

There exist two kinds of “unlike” recoupling resonances, namely, the resonances involving the motion of only one spin species, and the resonances involving both spin species. The resonances of the first kind are the following:

$$\omega = -\Omega_{ei} : \quad \omega = -\frac{\omega_{1i}^2 + \Omega_{0i}^2}{2\Omega_{0i}}, \quad (24)$$

$$\omega = \pm \frac{1}{2}\Omega_{ei} : \quad \omega = \frac{-\Omega_{0i} \pm \sqrt{4\Omega_{0i}^2 + 3\omega_{1i}^2}}{3}, \quad (25)$$

and also those obtained from Eq.(24,25) by replacing index i with index j . The resonances of the second kind are

$$\omega = (-1)^n \frac{1}{2}(\Omega_{ei} \pm \Omega_{ej}), \quad (26)$$

$$\omega = (-1)^n(\Omega_{ei} \pm \Omega_{ej}), \quad (27)$$

where variable n takes values 0 or 1 and thus controls the sign in front of the entire expression. Resonant conditions (26,27) lead to fourth-order polynomial equations with respect to ω , which, in principle can be solved analytically. However, in view of the cumbersome character of the resulting formulas, we chose to investigate the solutions numerically. Several plots illustrating the character of these solutions are presented in Fig. 4 and further in Fig. 5 of Appendix Appendix A. As evident from these plots, it cannot be guaranteed that each of the eight conditions envisioned by Eqs.(26,27) is realizable for a given set of values of γ_i , γ_j , H_0 and H_1 . For example, if $\gamma_i, \gamma_j > 0$, then no value of ω exists that would satisfy the condition $\omega = 1/2(\Omega_{ei} + \Omega_{ej})$.

The time-averaged Hamiltonians corresponding to the recoupling resonances (26,27) are the following:

$$\omega = -\Omega_{ei} : \quad \mathcal{H}_{D1}^u = \mathcal{H}_{D0}^u + \sum_{\langle i,j \rangle} J_{ij} \frac{3}{2} [\cos(\alpha_i + \alpha_j) - \cos \alpha_j] \left[-\frac{r_{ij,x}r_{ij,z}}{r_{ij}^2} I'_{ix}I'_{jz} + \frac{r_{ij,y}r_{ij,z}}{r_{ij}^2} I'_{iy}I'_{jz} \right], \quad (28)$$

$$\omega = \pm \frac{1}{2}\Omega_{ei} : \quad \mathcal{H}_{D2}^u = \mathcal{H}_{D0}^u + \sum_{\langle i,j \rangle} J_{ij} \frac{3}{4} [\sin \alpha_j (\cos \alpha_i \pm 1)] \left[\frac{r_{ij,y}^2 - r_{ij,x}^2}{r_{ij}^2} I'_{ix}I'_{jz} \mp \frac{2r_{ij,x}r_{ij,y}}{r_{ij}^2} I'_{iy}I'_{jz} \right], \quad (29)$$

$$\omega = (-1)^n(\Omega_{ei} \pm \Omega_{ej}) : \quad \mathcal{H}_{D3}^u = \mathcal{H}_{D0}^u + \sum_{\langle i,j \rangle} J_{ij} \frac{3}{4} [\sin(\alpha_i + \alpha_j) \pm (-1)^n \sin \alpha_i + (-1)^n \sin \alpha_j] \cdot \left[\frac{r_{ij,x}r_{ij,z}}{r_{ij}^2} (I'_{ix}I'_{jx} \mp I'_{iy}I'_{jy}) + (-1)^n \frac{r_{ij,y}r_{ij,z}}{r_{ij}^2} (\pm I'_{ix}I'_{jy} + I'_{iy}I'_{jx}) \right], \quad (30)$$

$$\omega = (-1)^n \frac{1}{2}(\Omega_{ei} \pm \Omega_{ej}) : \quad \mathcal{H}_{D4}^u = \mathcal{H}_{D0}^u + \sum_{\langle i,j \rangle} J_{ij} \frac{3}{8} [\cos \alpha_i + (-1)^n] [\cos \alpha_j \pm (-1)^n] \cdot \left[\frac{r_{ij,y}^2 - r_{ij,x}^2}{r_{ij}^2} (I'_{ix}I'_{jx} \mp I'_{iy}I'_{jy}) - (-1)^n \frac{2r_{ij,x}r_{ij,y}}{r_{ij}^2} (\pm I'_{ix}I'_{jy} + I'_{iy}I'_{jx}) \right]. \quad (31)$$

The upper (lower) sign of the recoupling resonances of

Eqs.(30,31) corresponds to the upper (lower) signs in the

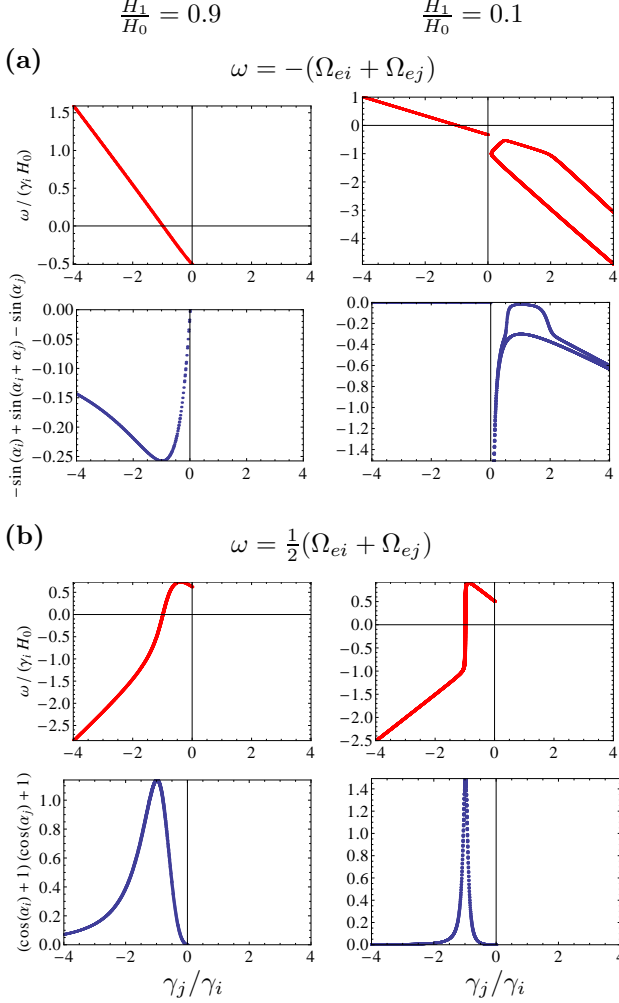


Figure 4: (Color online) Examples of recoupling resonances for unlike spins. Plots of the resonant values of ω and the prefactors in the recoupled Hamiltonians (30,31) as functions of γ_j/γ_i for two resonant conditions indicated above the respective plots. All examples presented are obtained numerically for either $H_1/H_0 = 0.9$ or $H_1/H_0 = 0.1$. Each column of plots corresponds to the ratio H_1/H_0 indicated above it. The plot lines consist of the actual computed points and thus in some cases have the appearance of dotted lines. The results for $H_1/H_0 = 0.1$ are qualitatively representative of the limit $H_1 \ll H_0$. The analogous plots for the six remaining resonant conditions associated with Eqs.(30,31) are given in Appendix Appendix A.

corresponding Hamiltonians. In the case of a small mismatch of the above resonant conditions, the additional term (15) for one or both spin species should be included. In the case of resonances (30,31), one, in fact, has the freedom of distributing the mismatch between the two spin species.

The standard truncated Hamiltonian (23) conserves both $\sum_i I'_{iz}$ and $\sum_j I'_{jz}$, while each of the recoupled Hamiltonians (28)-(31) violates the above conservation

for at least one of the two spin species. We observe, however, that the total z' -polarization of the both spin species, i.e. $\sum_i I'_{iz} + \sum_j I'_{jz}$, is still conserved by the recoupled Hamiltonians given by Eq.(30) for $\omega = \pm(\Omega_{ei} - \Omega_{ej})$ and by Eq.(31) for $\omega = \pm\frac{1}{2}(\Omega_{ei} - \Omega_{ej})$, because the terms in these Hamiltonians have the character of the so-called “flip-flops.”

In general, the recoupled Hamiltonians (24-27) are comparable to the standard truncated Hamiltonian (23), when H_1 is comparable to H_0 — see plots in Fig. 4 for $H_1/H_0 = 0.9$. If $H_1 \ll H_0$, then the recoupled terms are normally small, because Eq.(9) gives the values of α_i and α_j either close to 0 or to π — Figs. 5(c,d,f) for $H_1/H_0 = 0.1$.

However, as the plots in Figs. 4 and 5(a,b,e) for $H_1/H_0 = 0.1$ indicate, and our approximate calculations confirm, there are interesting and potentially useful exceptions, when the angle-dependent prefactors of the recoupled Hamiltonians remain comparable to 1 even though $H_1 \ll H_0$. The first exception corresponds to the condition $\gamma_j/\gamma_i \approx -1$ for the recoupling resonances $\omega = \pm 1/2(\Omega_{ei} - \Omega_{ej})$ and $\omega = 1/2(\Omega_{ei} + \Omega_{ej})$. In these cases, the recoupled terms in Hamiltonians (31) remain large as long as $|\gamma_j/\gamma_i + 1| \lesssim H_1/H_0$. [In the case of resonance $\omega = 1/2(\Omega_{ei} + \Omega_{ej})$, one should also be mindful of adding the secular double-flip contribution mentioned after Eq.(23).] This group of resonances can thus be exploited for pairs of nuclei satisfying the condition $\gamma_i \approx -\gamma_j$, such as e.g. ^{129}Xe and ^{23}Na . The second exception corresponds to the condition of $\gamma_j/\gamma_i \approx 0$ (or $\gamma_i/\gamma_j \approx 0$) for the resonances $\omega = \pm(\Omega_{ei} + \Omega_{ej})$. The corresponding recoupled Hamiltonians (30) are large, as long as $|\gamma_j/\gamma_i| \lesssim H_1/H_0$. These recoupling resonances can be very useful for the purposes of cross-polarization, when the gyromagnetic ratio of one of the two nuclei is much smaller than the other.

Finally, we mention that, as in the case of like spins, the suppression of the secular interaction terms between unlike spins by matching the magic angle condition or by the MAS technique is an additional resource for observing the recoupling resonances. The only difference in the present case is that the magic angle condition involves two angles: $3 \cos \alpha_i \cos \alpha_j - \cos(\alpha_i - \alpha_j) = 0$.

V. DISCUSSION

A. Experimental realizability

The standard truncated Hamiltonians (16,23) conserve the z' -projection of the total spin polarization for each of the available spin species in their respective double-rotated reference frames. The most obvious qualitative effect of the recoupled Hamiltonians is that they do not conserve this total z' -projection for at least one of the spin species. This difference can be tested experimentally. In the case of like spins, it will lead to the anomalously fast longitudinal relaxation discussed in Sec-

tion IV A. In the case of unlike spins, it may, in addition, lead to an anomalous cross-polarization effect.

To be specific, a possible way to observe the anomalous longitudinal relaxation can consist of the following steps: (i) polarizing the system in the static magnetic field; (ii) turning on the rf field (preferably, adiabatically) to match one of the recoupling resonance conditions; (iii) waiting enough time for the additional interaction terms to relax $\sum_i I'_{iz}$ (the waiting time should still be much shorter than T_1); and, finally, (iv) suddenly turning off the rf field. No free induction decay signal should be observable in this case. In contrast, away from the recoupling resonances, a free induction decay signal of finite intensity should always be observable for waiting times of the order of T_1 .

The requirements for the above kind of experiments are the following: (1) The static and the rf fields should be strong enough to ensure $\Omega_0, \omega_1 \gg 1/T_2$. (2) As discussed in the context of Eq.(15), the recoupling resonances should be matched to an accuracy of roughly $\frac{1}{T_2}$. (3) The static and the rf magnetic fields should be relatively homogeneous; otherwise the recoupling conditions cannot be satisfied over the entire sample. (4) The strength of the recoupled terms must be such that the timescale associated with the anomalous relaxation of the longitudinal magnetization is faster than T_1 (see the end of Section IV A). (5) Finally, in the case of $H_1 \sim H_0$, a real circularly polarized rf field should be used, as done, e.g., in Ref.¹³.

Now we discuss the observability of the recoupling resonances in the NMR setting that uses a linearly polarized rf field in the regime of $H_1 \ll H_0$. The latter condition extends to the experiments in larger static fields, which means stronger NMR signals.

The Hamiltonian averaging procedure used in this paper cannot be straightforwardly extended to linearly polarized rf fields, because a closed analytical solution for the spin motion is not available in such a case. In particular, the usual assumption that one can neglect one of the two counter-rotating components contributing to the linearly polarized rf field is not justified when $H_1 \sim H_0$. However, when $H_1 \ll H_0$, the case of linearly polarized rf field should be treatable by combining our truncation procedure with the perturbation expansion^{2,14}. In this limit, the presence of two rotating components may lead to additional recoupling resonances, but the resonances obtained in the present paper for a single rotating component of the same frequency should also be present. We further expect that the same recoupling resonance in the rotating and the linearly polarized settings is generically characterized by the same recoupled Hamiltonian, when the leading order of the expansion of this Hamiltonian in terms of H_1/H_0 is linear.

At small values of H_1/H_0 , the recoupling resonances satisfying the above linearity requirement are also the strongest and thus the most promising in terms of experimental observation. As discussed in Section IV A for the case of like spins, the linearity with respect to small H_1/H_0 is exhibited by some but not all recoupled Hamil-

tonians. We also note in this context, that an experiment with small linearly polarized fields should avoid the interplay with the secondary single-spin resonances described by Winter^{2,15}.)

In addition to the possibility of using stronger static fields and linearly polarized rf fields, the regime of $H_1 \ll H_0$ has two other advantages. First, the rf field homogeneity requirement is less stringent, when $H_1 \ll H_0$, because what matters is the homogeneity of the effective frequencies Ω_{ei} , to which the leading rf field contribution is only of the order of $(H_1/H_0)^2$. Second, in the case, when the secular part of the interaction is externally suppressed, the smallness of H_1/H_0 implies that the recoupling resonances can be resolved with higher accuracy (see the discussion in Section III).

B. Possible applications

Fundamental studies of spin-spin relaxation: Perhaps, the most direct use of the tunable Hamiltonians (20-22, 28-31) is to conduct fundamental experimental studies of nuclear spin-spin relaxation in solids, which is still not completely understood, in a much broader range of parameters than those accessible with the standard truncated Hamiltonians.

Cross-polarization: In the case of unlike spins, the recoupled Hamiltonians (30-31) for the resonances $\omega = \pm(\Omega_{ei} - \Omega_{ej})$ and $\omega = \pm\frac{1}{2}(\Omega_{ei} - \Omega_{ej})$ can be used to cross-polarize different spin species. As mentioned in Section IV B, these Hamiltonians contain “flip-flop” terms $I'_{ix}I'_{jy} - I'_{iy}I'_{jx}$ and $I'_{ix}I'_{jx} + I'_{iy}I'_{jy}$, which can transfer polarization from one spin species to the other. Such a transfer would require an rf field rotating with a single frequency, as opposed to the standard Hartmann-Hahn cross polarization routine¹⁶, which involves two rf-field frequencies. The two spin species can also be cross-polarized, albeit less efficiently, using the transient effect of the “double-flip” terms $I'_{ix}I'_{jy} + I'_{iy}I'_{jx}$ and $I'_{ix}I'_{jx} - I'_{iy}I'_{jy}$ for resonances $\omega = \pm(\Omega_{ei} + \Omega_{ej})$ and $\omega = \pm\frac{1}{2}(\Omega_{ei} + \Omega_{ej})$. The suppression of the secular terms by either the magic angle condition or the MAS technique, as discussed in section IV B, can enhance the efficiency of both the flip-flop-based and the double-flip-based cross-polarization processes. In the latter case this enhancement should be particularly significant.

Structure determination: The use of solid-state NMR for determining the structures of complex molecules involves MAS decoupling between nuclear spins followed by selective recoupling^{17,18}. The recoupling resonances obtained in this paper can, possibly, be used at the latter stage. As discussed in Section V A, the regime $H_1 \ll H_0$ may provide both the sufficient intensity and the sufficient frequency resolution for such experiments. If successful, such a method will not require the recoupling sequence to be adjusted to the sample spinning frequency. It will also have an added benefit of the non-trivial spatial dependence in the recoupled Hamiltonians as com-

pared to the usual secular interactions. This dependence can be converted into additional structure information for oriented samples.

In summary, the recoupling resonances for like and unlike spins amount to a new resource for manipulating nuclear spins, and, therefore, are likely to be useful for various NMR applications. However, the condition of applying a high amplitude rf field for a rather long time may be challenging to realize in practice.

VI. CONCLUSION

In this paper, we described theoretically the properties of recoupling resonances associated with the appearance of non-secular terms in the time-averaged Hamiltonians of nuclear spins-spin interaction in solids in the presence of strong rotating rf fields. Our analysis indicates that, under certain conditions, the effect of the recoupled non-secular interaction terms should be particularly well ob-

servable. We have also discussed the extension of our findings to the case of linearly polarized rf fields. Finally, we discussed how the recoupling resonances considered in this paper can be used for manipulating nuclear spins in various NMR applications.

Acknowledgments

We are grateful to J. Haase, J. Kohlrautz, B. Meier and C. P. Slichter for the discussions of this work.

Appendix A. PLOTS OF RECOUPLING RESONANCES FOR UNLIKE SPINS

This appendix contains the collection of plots (Fig. 5) for the six out of eight recoupling resonances described by Eqs.(30,31) that were not included in Fig. 4.

-
- * Electronic address: C.Kropf@thphys.uni-heidelberg.de
 - † Electronic address: B.Fine@thphys.uni-heidelberg.de
 - ¹ A. Redfield, *Physical Review* **98**, 1787 (1955).
 - ² A. Abragam, *Principles of Nuclear Magnetism* (Oxford University Press, Oxford, 1961).
 - ³ C. Slichter, *Principles of magnetic resonance* (Springer Verlag, New York, 1990).
 - ⁴ J. V. Vleck, *Physical Review* **74** (1948).
 - ⁵ T. G. Oas, R. Griffin, and M. Levitt, *J. Chem. Phys.* **89**, 692 (1988).
 - ⁶ J. M. Griffiths and R. G. Griffin, *Analytica Chimica Acta* **283**, 1081 (1993).
 - ⁷ Scholz, B. H. Meier, and M. Ernst, *J. Chem. Phys.* **127**, 204504 (2007).
 - ⁸ M. J. Bayro, M. Huber, R. Ramachandran, T. C. Davenport, B. H. Meier, M. Ernst, and R. G. Griffin, *J. Chem. Phys.* **130**, 114506 (2009).
 - ⁹ U. Haeberlen and J. S. Waugh, *Phys. Rev.* **175**, 453 (1968).
 - ¹⁰ V. I. Yukalov, *Phys. Rev. Lett.* **75**, 3000 (1995).
 - ¹¹ V. I. Yukalov, *Phys. Rev. B* **53**, 9232 (1996).
 - ¹² See the EPAPS supplemental material for the detailed description of the calculations used to obtain the time-averaged Hamiltonians presented in this paper.
 - ¹³ D. Sakellariou, C. A. Meriles, R. W. Martin, and A. Pines, *J. Magn. Res. Imag.* **23**, 295 (2005).
 - ¹⁴ F. Bloch and A. Siegert, *Phys. Rev.* **57**, 522 (1940).
 - ¹⁵ J. Winter, *C. R. Acad. Sci.* **241**, 375 (1955).
 - ¹⁶ S. Hartmann and E. Hahn, *Phys Review* **128**, 2042 (1962).
 - ¹⁷ C. P. Jaroniec, B. A. Tounage, C. M. Rienstra, J. Herzfeld, and R. G. Griffin, *J. Magn. Reson.* **146**, 132 (2000).
 - ¹⁸ C. P. Jaroniec, C. E. MacPhee, V. S. Bajaj, M. T. McMahon, and R. G. Griffin, *Proc. Natl. Acad. Sci.* **101**, 711 (2004).

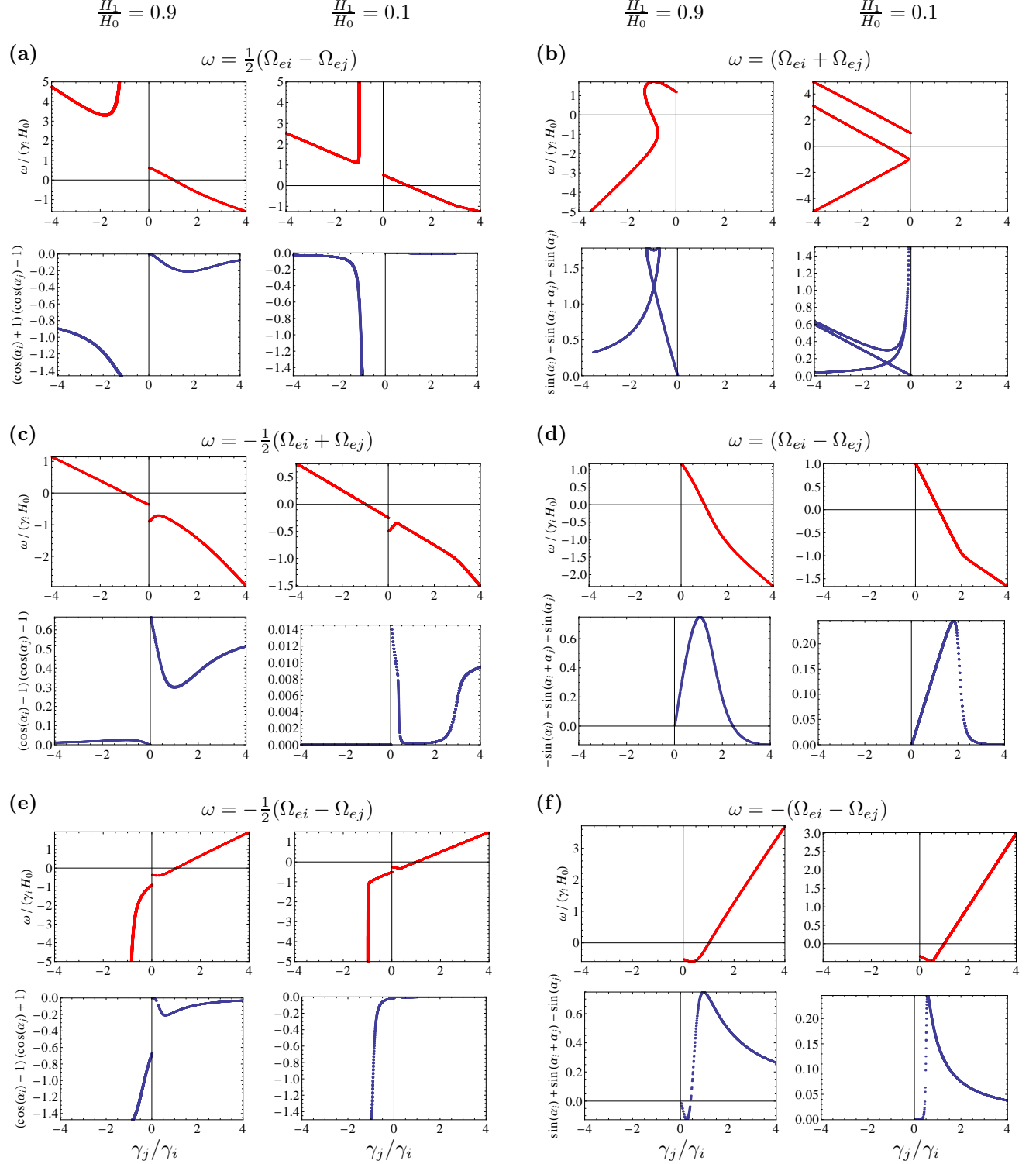


Figure 5: (Color online) Examples of recoupling resonances for unlike spins. Plots of the resonant values of ω and the prefactors in the recoupled Hamiltonians (30,31) as functions of γ_j/γ_i for the resonant conditions indicated above the respective plots. All examples presented are obtained numerically for either $H_1/H_0 = 0.9$ or $H_1/H_0 = 0.1$. Each column of plots corresponds to the ratio H_1/H_0 indicated above it. The plot lines consist of the actual computed points and thus in some cases have the appearance of dotted lines. The results for $H_1/H_0 = 0.1$ are qualitatively representative of the limit $H_1 \ll H_0$. The content of this figure together with Fig. 4 covers all eight resonant conditions associated with Eqs.(30,31)

SUPPLEMENTARY MATERIAL

Note 1: In this supplement, we use the same notations as in the main article unless explicitly specified otherwise.

Note 2: Some of the matrices in this supplement are computer-generated and presented as figures rather than equations.

S-I. FORMALISM FOR THE CALCULATIONS OF TIME-AVERAGED SPIN-SPIN INTERACTION HAMILTONIANS

We denote the full spin-spin interaction Hamiltonian in the double-rotated reference frame as $\mathcal{H}'_D(t)$. Our goal below is, first, to obtain the explicit expression for $\mathcal{H}'_D(t)$ and then to average it over time according to formula

$$\langle \mathcal{H}'_D \rangle = \lim_{\tau \rightarrow \infty} \frac{1}{2\tau} \int_{-\tau}^{\tau} \mathcal{H}'_D(t) dt. \quad (\text{S1})$$

The Hamiltonian $\mathcal{H}'_D(t)$ can be represented in tensor notations as follows

$$\mathcal{H}'_D(t) = \sum_{i < j}^N J_{ij} \cdot I'_{i,\mu} A_{\mu\nu}(ij)_{\mu\nu} I'_{j,\nu}, \quad (\text{S2})$$

where we use the Einstein convention for summing over repeated Greek-letter matrix and vector indices, which can take values 1, 2, 3 and correspond, respectively, to the x, y, z projections in the relevant reference frame. The matrix $A_{\mu\nu}(ij)$ is given by the following equation:

$$A_{\mu\nu}(ij) = P_{\mu\delta}(i) C_{\delta\rho}(ij) Q_{\rho\nu}(j), \quad (\text{S3})$$

where time-independent matrix $C_{\mu\nu}(ij)$ represents the interaction coefficients of the full interaction Hamiltonian \mathcal{H}_D in the laboratory reference frame, while time-dependent matrices $P_{\mu\nu}(i)$ and $Q_{\mu\nu}(j)$ represent the transformations between the laboratory and the double-rotated reference frames appropriate for spins i or j , respectively. Matrix $C_{\mu\nu}(ij)$ is presented in Fig. S1.

$1 - 3 n_{ij,x}^2$	$-3 n_{ij,x} n_{ij,y}$	$-3 n_{ij,x} n_{ij,z}$
Sym	$1 - 3 n_{ij,y}^2$	$-3 n_{ij,y} n_{ij,z}$
Sym	Sym	$1 - 3 n_{ij,z}^2$

Figure S1: Explicit form of the matrix $C_{\mu\nu}(ij)$. The factors $n_{ij,\mu} = \frac{r_{i,\mu}}{|r_{ij}|}$ are time-independent material constants. The matrix $C_{\mu\nu}(ij)$ is symmetric.

The expressions for the transformation matrices are:

$$P_{\mu\nu}(i) = U_{\Omega_{ei}, \mu\delta, \mu\nu} U_{\alpha i, \delta\rho} U_{\omega, \rho\nu}, \quad (\text{S4})$$

and

$$Q_{\mu\nu}(j)_{\mu\nu} = U_{\omega, \mu\delta}^T U_{\alpha j, \delta\rho}^T U_{\Omega_{ej}, \rho\nu}^T, \quad (\text{S5})$$

where

$$U_{\omega,\mu\nu} = \begin{pmatrix} \cos(\omega t) & \sin(\omega t) & 0 \\ -\sin(\omega t) & \cos(\omega t) & 0 \\ 0 & 0 & 1 \end{pmatrix}, \quad (\text{S6})$$

$$U_{\alpha_i,\mu\nu} = \begin{pmatrix} \cos(\alpha_i) & 0 & -\sin(\alpha_i) \\ 0 & 1 & 0 \\ \sin(\alpha_i) & 0 & \cos(\alpha_i) \end{pmatrix}, \quad (\text{S7})$$

$$U_{\Omega_{ei},\mu\nu} = \begin{pmatrix} \cos(\Omega_{ei} \cdot t) & -\sin(\Omega_{ei} \cdot t) & 0 \\ \sin(\Omega_{ei} \cdot t) & \cos(\Omega_{ei,j} \cdot t) & 0 \\ 0 & 0 & 1 \end{pmatrix}. \quad (\text{S8})$$

These are the same matrices as those defined by Eqs.(7-9) of the main article but with the spin and matrix indices explicitly included. The explicit form of matrices $P_{\mu\nu}(i)$ and $Q_{\mu\nu}(j)$ is given in Figs. S2 and S3, respectively.

$\text{Cos}[\mathfrak{t} \, \omega] \, \text{Cos}[\alpha_i] \, \text{Cos}[\mathfrak{t} \, \Omega_{ei}] +$ $\text{Sin}[\mathfrak{t} \, \omega] \, \text{Sin}[\mathfrak{t} \, \Omega_{ei}]$	$\text{Cos}[\alpha_i] \, \text{Cos}[\mathfrak{t} \, \Omega_{ei}] \, \text{Sin}[\mathfrak{t} \, \omega] -$ $\text{Cos}[\mathfrak{t} \, \omega] \, \text{Sin}[\mathfrak{t} \, \Omega_{ei}]$	$-\text{Cos}[\mathfrak{t} \, \Omega_{ei}] \, \text{Sin}[\alpha_i]$
$-\text{Cos}[\mathfrak{t} \, \Omega_{ei}] \, \text{Sin}[\mathfrak{t} \, \omega] +$ $\text{Cos}[\mathfrak{t} \, \omega] \, \text{Cos}[\alpha_i] \, \text{Sin}[\mathfrak{t} \, \Omega_{ei}]$	$\text{Cos}[\mathfrak{t} \, \omega] \, \text{Cos}[\mathfrak{t} \, \Omega_{ei}] +$ $\text{Cos}[\alpha_i] \, \text{Sin}[\mathfrak{t} \, \omega] \, \text{Sin}[\mathfrak{t} \, \Omega_{ei}]$	$-\text{Sin}[\alpha_i] \, \text{Sin}[\mathfrak{t} \, \Omega_{ei}]$
$\text{Cos}[\mathfrak{t} \, \omega] \, \text{Sin}[\alpha_i]$	$\text{Sin}[\mathfrak{t} \, \omega] \, \text{Sin}[\alpha_i]$	$\text{Cos}[\alpha_i]$

Figure S2: Explicit form of the matrix $P_{\mu\nu}(i)$

$\text{Cos}[\mathfrak{t} \, \omega] \, \text{Cos}[\alpha_j] \, \text{Cos}[\mathfrak{t} \, \Omega_{ej}] +$ $\text{Sin}[\mathfrak{t} \, \omega] \, \text{Sin}[\mathfrak{t} \, \Omega_{ej}]$	$-\text{Cos}[\mathfrak{t} \, \Omega_{ej}] \, \text{Sin}[\mathfrak{t} \, \omega] +$ $\text{Cos}[\mathfrak{t} \, \omega] \, \text{Cos}[\alpha_j] \, \text{Sin}[\mathfrak{t} \, \Omega_{ej}]$	$\text{Cos}[\mathfrak{t} \, \omega] \, \text{Sin}[\alpha_j]$
$\text{Cos}[\alpha_j] \, \text{Cos}[\mathfrak{t} \, \Omega_{ej}] \, \text{Sin}[\mathfrak{t} \, \omega] -$ $\text{Cos}[\mathfrak{t} \, \omega] \, \text{Sin}[\mathfrak{t} \, \Omega_{ej}]$	$\text{Cos}[\mathfrak{t} \, \omega] \, \text{Cos}[\mathfrak{t} \, \Omega_{ej}] +$ $\text{Cos}[\alpha_j] \, \text{Sin}[\mathfrak{t} \, \omega] \, \text{Sin}[\mathfrak{t} \, \Omega_{ej}]$	$\text{Sin}[\mathfrak{t} \, \omega] \, \text{Sin}[\alpha_j]$
$-\text{Cos}[\mathfrak{t} \, \Omega_{ej}] \, \text{Sin}[\alpha_j]$	$-\text{Sin}[\alpha_j] \, \text{Sin}[\mathfrak{t} \, \Omega_{ej}]$	$\text{Cos}[\alpha_j]$

Figure S3: Explicit form of the matrix $Q_{\mu\nu}(j)$

The calculation of the time-average of $\mathcal{H}'_D(t)$ given by Eq.(S1) requires calculating

$$\langle A_{\mu\nu}(ij) \rangle = \lim_{\tau \rightarrow \infty} \frac{1}{2\tau} \int_{-\tau}^{\tau} A_{\mu\nu}(ij)(t) dt \quad (\text{S9})$$

The full and time-averaged expressions for matrix $A_{\mu\nu}(ij)(t)$ are presented, for the case of like spins, in Section S-II and, for the case of unlike spins, in Section S-III.

To describe the different recoupling resonances we use “normalized delta-function” symbol $\delta(x)$ defined as follows:

$$\delta(x) = \begin{cases} 1 & \text{if } x = 0; \\ 0 & \text{otherwise.} \end{cases} \quad (\text{S10})$$

S-II. LIKE SPINS

For like spins, we use the notation

$$\alpha_i = \alpha_j \equiv \alpha \quad (\text{S11})$$

and

$$\Omega_{ei} = \Omega_{ej} \equiv \Omega_e. \quad (\text{S12})$$

In this case, $P_{\mu\nu}(i) = Q_{\mu\nu}(j)$, and, as a result, $A_{\mu\nu}(ij)$ is symmetric. The time-dependent matrix $A_{\mu\nu}(ij)$ is presented in function of the elements of $C_{\mu\nu}(ij)$, $P_{\mu\nu}(i)$ and $Q_{\mu\nu}(j)$ in Fig. S4. The explicit form of $A_{\mu\nu}(ij)$ as a function of α , ω and Ω_e is given in Fig. S5. The time-averaged value of $A_{\mu\nu}(ij)$ is presented in Fig. S6.

$P_{11} (C_{11} P_{11} + C_{12} P_{21} + C_{13} P_{31}) +$ $P_{21} (C_{12} P_{11} + C_{22} P_{21} + C_{23} P_{31}) +$ $P_{31} (C_{13} P_{11} + C_{23} P_{21} + C_{33} P_{31})$	$P_{12} (C_{11} P_{11} + C_{12} P_{21} + C_{13} P_{31}) +$ $P_{22} (C_{12} P_{11} + C_{22} P_{21} + C_{23} P_{31}) +$ $(C_{13} P_{11} + C_{23} P_{21} + C_{33} P_{31}) P_{32}$	$P_{13} (C_{11} P_{11} + C_{12} P_{21} + C_{13} P_{31}) +$ $P_{23} (C_{12} P_{11} + C_{22} P_{21} + C_{23} P_{31}) +$ $(C_{13} P_{11} + C_{23} P_{21} + C_{33} P_{31}) P_{33}$
Sym	$P_{12} (C_{11} P_{12} + C_{12} P_{22} + C_{13} P_{32}) +$ $P_{22} (C_{12} P_{12} + C_{22} P_{22} + C_{23} P_{32}) +$ $P_{32} (C_{13} P_{12} + C_{23} P_{22} + C_{33} P_{32})$	$P_{13} (C_{11} P_{12} + C_{12} P_{22} + C_{13} P_{32}) +$ $P_{23} (C_{12} P_{12} + C_{22} P_{22} + C_{23} P_{32}) +$ $(C_{13} P_{12} + C_{23} P_{22} + C_{33} P_{32}) P_{33}$
Sym	Sym	$P_{13} (C_{11} P_{13} + C_{12} P_{23} + C_{13} P_{33}) +$ $P_{23} (C_{12} P_{13} + C_{22} P_{23} + C_{23} P_{33}) +$ $P_{33} (C_{13} P_{13} + C_{23} P_{23} + C_{33} P_{33})$

Figure S4: Like spins : The matrix $A_{\mu\nu}(ij)$ in compact form. Here $C_{\mu\nu} \equiv C_{\mu\nu}(ij)$, $P_{\mu\nu} \equiv P_{\mu\nu}(i)$ and $Q_{\mu\nu} \equiv Q_{\mu\nu}(j)$.

$\begin{aligned} & \cos[\alpha]^2 \cos[t\omega]^2 \cos[t\Omega_e]^2 C_{11} + \\ & 2 \cos[\alpha] \cos[t\omega] \cos[t\Omega_e] \sin[t\omega] \sin[t\Omega_e] C_{11} + \\ & \sin[t\omega]^2 \sin[t\Omega_e]^2 C_{11} + \\ & 2 \cos[\alpha]^2 \cos[t\omega] \cos[t\Omega_e]^2 \sin[t\omega] C_{12} - \\ & 2 \cos[\alpha] \cos[t\omega]^2 \cos[t\Omega_e] \sin[t\Omega_e] C_{12} + \\ & 2 \cos[\alpha] \cos[t\Omega_e] \sin[t\omega]^2 \sin[t\Omega_e] C_{12} - \\ & 2 \cos[t\omega] \sin[t\omega] \sin[t\Omega_e]^2 C_{12} - \\ & 2 \cos[\alpha] \cos[t\omega] \cos[t\Omega_e]^2 \sin[\alpha] C_{13} - \\ & 2 \cos[t\Omega_e] \sin[\alpha] \sin[t\omega] \sin[t\Omega_e] C_{13} + \\ & \cos[\alpha]^2 \cos[t\Omega_e]^2 \sin[t\omega]^2 C_{22} - \\ & 2 \cos[\alpha] \cos[t\omega] \cos[t\Omega_e] \sin[t\omega] \sin[t\Omega_e] C_{22} + \\ & \cos[t\omega]^2 \sin[t\Omega_e]^2 C_{22} - \\ & 2 \cos[\alpha] \cos[t\Omega_e]^2 \sin[\alpha] \sin[t\omega] C_{23} + \\ & 2 \cos[t\omega] \cos[t\Omega_e] \sin[\alpha] \sin[t\Omega_e] C_{23} + \\ & \cos[t\Omega_e]^2 \sin[\alpha]^2 C_{33} \end{aligned}$	$\begin{aligned} & -\cos[\alpha] \cos[t\omega] \cos[t\Omega_e]^2 \sin[t\omega] C_{11} + \\ & \cos[\alpha]^2 \cos[t\omega]^2 \cos[t\Omega_e] \sin[t\Omega_e] C_{11} - \\ & \cos[t\Omega_e] \sin[t\omega]^2 \sin[t\Omega_e] C_{11} + \\ & \cos[\alpha] \cos[t\omega] \sin[t\omega] \sin[t\Omega_e]^2 C_{11} + \\ & \cos[\alpha] \cos[t\omega]^2 \cos[t\Omega_e]^2 C_{12} - \\ & \cos[\alpha] \cos[t\Omega_e]^2 \sin[t\omega]^2 C_{12} + \\ & 2 \cos[t\omega] \cos[t\Omega_e] \sin[t\omega] \sin[t\Omega_e] C_{12} + \\ & 2 \cos[\alpha]^2 \cos[t\omega] \cos[t\Omega_e] \sin[t\omega] \sin[t\Omega_e] C_{12} - \\ & \cos[\alpha] \cos[t\omega]^2 \sin[t\Omega_e]^2 C_{12} + \\ & \cos[\alpha] \sin[t\omega]^2 \sin[t\Omega_e]^2 C_{12} + \\ & \cos[t\Omega_e] \sin[\alpha] \sin[t\omega] C_{13} - \\ & 2 \cos[\alpha] \cos[t\omega] \cos[t\Omega_e] \sin[\alpha] \sin[t\Omega_e] C_{13} - \\ & \sin[\alpha] \sin[t\omega] \sin[t\Omega_e]^2 C_{13} + \\ & \cos[\alpha] \cos[t\omega] \cos[t\Omega_e]^2 \sin[t\omega] C_{22} - \\ & \cos[t\omega]^2 \cos[t\Omega_e] \sin[t\Omega_e] C_{22} + \\ & \cos[\alpha]^2 \cos[t\Omega_e] \sin[t\omega]^2 \sin[t\Omega_e] C_{22} - \\ & \cos[\alpha] \cos[t\omega] \sin[t\omega] \sin[t\Omega_e]^2 C_{22} - \\ & \cos[t\omega] \cos[t\Omega_e]^2 \sin[\alpha] C_{23} - \\ & 2 \cos[\alpha] \cos[t\Omega_e] \sin[\alpha] \sin[t\omega] \sin[t\Omega_e] C_{23} + \\ & \cos[t\omega] \sin[\alpha] \sin[t\Omega_e]^2 C_{23} + \\ & \cos[t\Omega_e] \sin[\alpha]^2 \sin[t\Omega_e] C_{33} \end{aligned}$	$\begin{aligned} & \cos[\alpha] \cos[t\omega]^2 \cos[t\Omega_e] \sin[\alpha] C_{11} + \\ & \cos[t\omega] \sin[\alpha] \sin[t\omega] \sin[t\Omega_e] C_{11} + \\ & 2 \cos[\alpha] \cos[t\omega] \cos[t\Omega_e] \sin[\alpha] \sin[t\omega] C_{12} - \\ & \cos[t\omega]^2 \sin[\alpha] \sin[t\Omega_e] C_{12} + \\ & \sin[\alpha] \sin[t\omega]^2 \sin[t\Omega_e] C_{12} + \\ & \cos[\alpha]^2 \cos[t\omega] \cos[t\Omega_e] C_{13} - \\ & \cos[t\omega] \cos[t\Omega_e] \sin[\alpha]^2 C_{13} + \\ & \cos[\alpha] \sin[t\omega] \sin[t\Omega_e] C_{13} + \\ & \cos[\alpha] \cos[t\Omega_e] \sin[\alpha] \sin[t\omega]^2 C_{22} - \\ & \cos[t\omega] \sin[\alpha] \sin[t\omega] \sin[t\Omega_e] C_{22} + \\ & \cos[\alpha]^2 \cos[t\Omega_e] \sin[t\omega] C_{23} - \\ & \cos[t\Omega_e] \sin[\alpha]^2 \sin[t\omega] C_{23} - \\ & \cos[\alpha] \cos[t\omega] \sin[t\Omega_e] C_{23} - \\ & \cos[\alpha] \cos[t\Omega_e] \sin[\alpha] C_{33} \end{aligned}$
Sym	$\begin{aligned} & \cos[t\Omega_e]^2 \sin[t\omega]^2 C_{11} - \\ & 2 \cos[\alpha] \cos[t\omega] \cos[t\Omega_e] \sin[t\omega] \sin[t\Omega_e] C_{11} + \\ & \cos[\alpha]^2 \cos[t\omega]^2 \sin[t\Omega_e]^2 C_{11} - \\ & 2 \cos[t\omega] \cos[t\Omega_e]^2 \sin[t\omega] C_{12} + \\ & 2 \cos[\alpha] \cos[t\omega]^2 \cos[t\Omega_e] \sin[t\Omega_e] C_{12} - \\ & 2 \cos[\alpha] \cos[t\Omega_e] \sin[t\omega]^2 \sin[t\Omega_e] C_{12} + \\ & 2 \cos[\alpha]^2 \cos[t\omega] \sin[t\omega] \sin[t\Omega_e]^2 C_{12} + \\ & 2 \cos[t\Omega_e] \sin[\alpha] \sin[t\omega] \sin[t\Omega_e] C_{13} - \\ & 2 \cos[\alpha] \cos[t\omega] \sin[\alpha] \sin[t\Omega_e]^2 C_{13} + \\ & \cos[t\omega]^2 \cos[t\Omega_e]^2 C_{22} + \\ & 2 \cos[\alpha] \cos[t\omega] \cos[t\Omega_e] \sin[t\omega] \sin[t\Omega_e] C_{22} + \\ & \cos[\alpha]^2 \sin[t\omega]^2 \sin[t\Omega_e]^2 C_{22} - \\ & 2 \cos[t\omega] \cos[t\Omega_e] \sin[\alpha] \sin[t\Omega_e] C_{23} - \\ & 2 \cos[\alpha] \sin[\alpha] \sin[t\omega] \sin[t\Omega_e]^2 C_{23} + \\ & \sin[\alpha]^2 \sin[t\Omega_e]^2 C_{33} \end{aligned}$	$\begin{aligned} & -\cos[t\omega] \cos[t\Omega_e] \sin[\alpha] \sin[t\omega] C_{11} + \\ & \cos[\alpha] \cos[t\omega]^2 \sin[\alpha] \sin[t\Omega_e] C_{11} + \\ & \cos[t\omega]^2 \cos[t\Omega_e] \sin[\alpha] C_{12} - \\ & \cos[t\Omega_e] \sin[\alpha] \sin[t\omega]^2 C_{12} + \\ & 2 \cos[\alpha] \cos[t\omega] \sin[\alpha] \sin[t\omega] \sin[t\Omega_e] C_{12} - \\ & \cos[\alpha] \cos[t\Omega_e] \sin[t\omega] C_{13} + \\ & \cos[\alpha]^2 \cos[t\omega] \sin[t\Omega_e] C_{13} - \\ & \cos[t\omega] \sin[\alpha]^2 \sin[t\Omega_e] C_{13} + \\ & \cos[t\omega] \cos[t\Omega_e] \sin[\alpha] \sin[t\omega] C_{22} + \\ & \cos[\alpha] \sin[\alpha] \sin[t\omega]^2 \sin[t\Omega_e] C_{22} + \\ & \cos[\alpha] \cos[t\omega] \cos[t\Omega_e] C_{23} + \\ & \cos[\alpha]^2 \sin[t\omega] \sin[t\Omega_e] C_{23} - \\ & \sin[\alpha]^2 \sin[t\omega] \sin[t\Omega_e] C_{23} - \\ & \cos[\alpha] \sin[\alpha] \sin[t\Omega_e] C_{33} \end{aligned}$
Sym	Sym	$\begin{aligned} & \cos[t\omega]^2 \sin[\alpha]^2 C_{11} + \\ & 2 \cos[t\omega] \sin[\alpha]^2 \sin[t\omega] C_{12} + \\ & 2 \cos[\alpha] \cos[t\omega] \sin[\alpha] C_{13} + \\ & \sin[\alpha]^2 \sin[t\omega]^2 C_{22} + \\ & 2 \cos[\alpha] \sin[\alpha] \sin[t\omega] C_{23} + \cos[\alpha]^2 C_{33} \end{aligned}$

Figure S5: Like spins : Explicit form of the matrix $A_{\mu\nu}(ij)$

$\begin{aligned} & \left(\frac{1}{4} + \frac{\cos[\alpha]^2}{4} \right) C_{11} + \\ & \frac{1}{4} \delta(\omega+2\Omega_e) (2 \sin[\alpha] - \sin[2\alpha]) C_{13} + \\ & \frac{1}{8} \delta(\omega+\Omega_e) (-1 + \cos[\alpha])^2 (C_{11} - C_{22}) + \\ & \left(\frac{1}{4} + \frac{\cos[\alpha]^2}{4} \right) C_{22} + \frac{1}{2} \sin[\alpha]^2 C_{33} \end{aligned}$	$\begin{aligned} & -\frac{1}{4} \delta(\omega+\Omega_e) (-1 + \cos[\alpha])^2 C_{12} + \\ & \frac{1}{4} \delta(\omega+2\Omega_e) (-2 \sin[\alpha] + \sin[2\alpha]) C_{23} \end{aligned}$	$\begin{aligned} & \frac{1}{2} \delta(\omega+\Omega_e) (-\cos[\alpha] + \cos[\alpha]^2 - \sin[\alpha]^2) C_{13} - \\ & \frac{1}{8} \delta(2\omega+\Omega_e) (2 \sin[\alpha] - \sin[2\alpha]) (C_{11} - C_{22}) + \\ & \frac{1}{8} \delta(2\omega-\Omega_e) (2 \sin[\alpha] + \sin[2\alpha]) (C_{11} - C_{22}) \end{aligned}$
Sym	$\begin{aligned} & \left(\frac{1}{4} + \frac{\cos[\alpha]^2}{4} \right) C_{11} + \\ & \frac{1}{4} \delta(\omega+2\Omega_e) (-2 \sin[\alpha] + \sin[2\alpha]) C_{13} - \\ & \frac{1}{8} \delta(\omega+\Omega_e) (-1 + \cos[\alpha])^2 (C_{11} - C_{22}) + \\ & \left(\frac{1}{4} + \frac{\cos[\alpha]^2}{4} \right) C_{22} + \frac{1}{2} \sin[\alpha]^2 C_{33} \end{aligned}$	$\begin{aligned} & \frac{1}{4} \delta(2\omega+\Omega_e) (2 \sin[\alpha] - \sin[2\alpha]) C_{12} + \\ & \frac{1}{4} \delta(2\omega-\Omega_e) (2 \sin[\alpha] + \sin[2\alpha]) C_{12} + \\ & \frac{1}{2} \delta(\omega+\Omega_e) (\cos[\alpha] - \cos[\alpha]^2 + \sin[\alpha]^2) C_{23} \end{aligned}$
Sym	Sym	$\frac{1}{2} \sin[\alpha]^2 C_{11} + \frac{1}{2} \sin[\alpha]^2 C_{22} + \cos[\alpha]^2 C_{33}$

Figure S6: Like spins : Time average of the matrix $A_{\mu\nu}(ij)$. All time-averaged Hamiltonians for like spins presented in Section IVA of the main article follow from this expression.

S-III. UNLIKE SPINS

For unlike spins, $\gamma_i \neq \gamma_j$. The main article associates indices i and j with two different spin species. In this section, in order to make formulas better readable, we change the notations as follows:

$$\alpha_i \equiv \alpha \quad (\text{S13})$$

$$\alpha_j \equiv \beta \quad (\text{S14})$$

$$\Omega_{ei} \equiv \Omega. \quad (\text{S15})$$

$$\Omega_{ej} \equiv \Lambda. \quad (\text{S16})$$

In the present case, $P_{\mu\nu}(i) \neq Q_{\mu\nu}(j)$, and, therefore, $A_{\mu\nu}(ij)$ is not symmetric. The time-dependent matrix $A_{\mu\nu}(ij)$ is presented as a function of $C_{\mu\nu}(ij)$, $P_{\mu\nu}(i)$ and $Q_{\mu\nu}(j)$ in Fig. S7. The explicit form of $A_{\mu\nu}(ij)$ as a function of α , β , ω , Ω and Λ is given in Fig. S8. The result of time-averaging for $A_{\mu\nu}(ij)$ is presented in Fig. S9.

$P_{11} (C_{11} Q_{11} + C_{12} Q_{21} + C_{13} Q_{31}) +$ $P_{21} (C_{12} Q_{11} + C_{22} Q_{21} + C_{23} Q_{31}) +$ $P_{31} (C_{13} Q_{11} + C_{23} Q_{21} + C_{33} Q_{31})$	$P_{12} (C_{11} Q_{11} + C_{12} Q_{21} + C_{13} Q_{31}) +$ $P_{22} (C_{12} Q_{11} + C_{22} Q_{21} + C_{23} Q_{31}) +$ $P_{32} (C_{13} Q_{11} + C_{23} Q_{21} + C_{33} Q_{31})$	$P_{13} (C_{11} Q_{11} + C_{12} Q_{21} + C_{13} Q_{31}) +$ $P_{23} (C_{12} Q_{11} + C_{22} Q_{21} + C_{23} Q_{31}) +$ $P_{33} (C_{13} Q_{11} + C_{23} Q_{21} + C_{33} Q_{31})$
$P_{11} (C_{11} Q_{12} + C_{12} Q_{22} + C_{13} Q_{32}) +$ $P_{21} (C_{12} Q_{12} + C_{22} Q_{22} + C_{23} Q_{32}) +$ $P_{31} (C_{13} Q_{12} + C_{23} Q_{22} + C_{33} Q_{32})$	$P_{12} (C_{11} Q_{12} + C_{12} Q_{22} + C_{13} Q_{32}) +$ $P_{22} (C_{12} Q_{12} + C_{22} Q_{22} + C_{23} Q_{32}) +$ $P_{32} (C_{13} Q_{12} + C_{23} Q_{22} + C_{33} Q_{32})$	$P_{13} (C_{11} Q_{12} + C_{12} Q_{22} + C_{13} Q_{32}) +$ $P_{23} (C_{12} Q_{12} + C_{22} Q_{22} + C_{23} Q_{32}) +$ $P_{33} (C_{13} Q_{12} + C_{23} Q_{22} + C_{33} Q_{32})$
$P_{11} (C_{11} Q_{13} + C_{12} Q_{23} + C_{13} Q_{33}) +$ $P_{21} (C_{12} Q_{13} + C_{22} Q_{23} + C_{23} Q_{33}) +$ $P_{31} (C_{13} Q_{13} + C_{23} Q_{23} + C_{33} Q_{33})$	$P_{12} (C_{11} Q_{13} + C_{12} Q_{23} + C_{13} Q_{33}) +$ $P_{22} (C_{12} Q_{13} + C_{22} Q_{23} + C_{23} Q_{33}) +$ $P_{32} (C_{13} Q_{13} + C_{23} Q_{23} + C_{33} Q_{33})$	$P_{13} (C_{11} Q_{13} + C_{12} Q_{23} + C_{13} Q_{33}) +$ $P_{23} (C_{12} Q_{13} + C_{22} Q_{23} + C_{23} Q_{33}) +$ $P_{33} (C_{13} Q_{13} + C_{23} Q_{23} + C_{33} Q_{33})$

Figure S7: Unlike spins : The matrix $A_{\mu\nu}(ij)$ in compact form. Here $C_{\mu\nu} \equiv C_{\mu\nu}(ij)$, $P_{\mu\nu} \equiv P_{\mu\nu}(i)$ and $Q_{\mu\nu} \equiv Q_{\mu\nu}(j)$.

Figure S8: Unlike spins : Explicit form of the matrix $A_{\mu\nu}(ij)$

$ \begin{aligned} & -\frac{1}{4} \delta(\omega + (\Omega + \Lambda)) ((-1 + \cos[\beta]) \sin[\alpha] + (-1 + \cos[\alpha]) \sin[\beta]) C_{13} - \\ & \frac{1}{4} \delta(\omega + (\Omega - \Lambda)) ((1 + \cos[\beta]) \sin[\alpha] + (-1 + \cos[\alpha]) \sin[\beta]) C_{13} - \\ & \frac{1}{4} \delta(\omega - (\Omega - \Lambda)) ((-1 + \cos[\beta]) \sin[\alpha] + (1 + \cos[\alpha]) \sin[\beta]) C_{13} - \\ & \frac{1}{4} \delta(\omega - (\Omega + \Lambda)) ((1 + \cos[\beta]) \sin[\alpha] + (1 + \cos[\alpha]) \sin[\beta]) C_{13} + \\ & \frac{1}{8} \delta(2\omega - (\Omega + \Lambda)) (-1 + \cos[\alpha]) (-1 + \cos[\beta]) (C_{11} - C_{22}) + \\ & \frac{1}{8} \delta(2\omega - (\Omega - \Lambda)) (1 + \cos[\alpha]) (-1 + \cos[\beta]) (C_{11} - C_{22}) + \\ & \frac{1}{8} \delta(2\omega + (\Omega - \Lambda)) (-1 + \cos[\alpha]) (1 + \cos[\beta]) (C_{11} - C_{22}) + \\ & \frac{1}{8} \delta(2\omega - (\Omega + \Lambda)) (1 + \cos[\alpha]) (1 + \cos[\beta]) (C_{11} - C_{22}) \end{aligned} $	$ \begin{aligned} & -\frac{1}{4} \delta(2\omega - (\Omega + \Lambda)) (-1 + \cos[\alpha]) (-1 + \cos[\beta]) C_{12} - \\ & \frac{1}{4} \delta(2\omega - (\Omega - \Lambda)) (1 + \cos[\alpha]) (-1 + \cos[\beta]) C_{12} + \\ & \frac{1}{4} \delta(2\omega + (\Omega - \Lambda)) (-1 + \cos[\alpha]) (1 + \cos[\beta]) C_{12} + \\ & \frac{1}{4} \delta(2\omega - (\Omega + \Lambda)) (1 + \cos[\alpha]) (1 + \cos[\beta]) C_{12} + \\ & \frac{1}{4} \delta(\omega + (\Omega + \Lambda)) ((-1 + \cos[\beta]) \sin[\alpha] + (-1 + \cos[\alpha]) \sin[\beta]) C_{23} - \\ & \frac{1}{4} \delta(\omega + (\Omega - \Lambda)) ((1 + \cos[\beta]) \sin[\alpha] + (-1 + \cos[\alpha]) \sin[\beta]) C_{23} + \\ & \frac{1}{4} \delta(\omega - (\Omega - \Lambda)) ((-1 + \cos[\beta]) \sin[\alpha] + (1 + \cos[\alpha]) \sin[\beta]) C_{23} - \\ & \frac{1}{4} \delta(\omega - (\Omega + \Lambda)) ((1 + \cos[\beta]) \sin[\alpha] + (1 + \cos[\alpha]) \sin[\beta]) C_{23} \end{aligned} $	$ \begin{aligned} & \frac{1}{2} \delta(\omega + \Omega_{\text{el}}) \\ & ((-1 + \cos[\alpha]) \cos[\beta] - \sin[\alpha] \sin[\beta]) C_{13} + \\ & \frac{1}{4} \delta(2\omega + \Omega_{\text{el}}) (-1 + \cos[\alpha]) \sin[\beta] (C_{11} - C_{22}) + \\ & \frac{1}{4} \delta(2\omega - \Omega_{\text{el}}) (1 + \cos[\alpha]) \sin[\beta] (C_{11} - C_{22}) \end{aligned} $
$ \begin{aligned} & -\frac{1}{4} \delta(2\omega - (\Omega + \Lambda)) (-1 + \cos[\alpha]) (-1 + \cos[\beta]) C_{12} + \\ & \frac{1}{4} \delta(2\omega - (\Omega - \Lambda)) (1 + \cos[\alpha]) (-1 + \cos[\beta]) C_{12} - \\ & \frac{1}{4} \delta(2\omega + (\Omega - \Lambda)) (-1 + \cos[\alpha]) (1 + \cos[\beta]) C_{12} + \\ & \frac{1}{4} \delta(2\omega - (\Omega + \Lambda)) (1 + \cos[\alpha]) (1 + \cos[\beta]) C_{12} + \\ & \frac{1}{4} \delta(\omega + (\Omega + \Lambda)) ((-1 + \cos[\beta]) \sin[\alpha] + (-1 + \cos[\alpha]) \sin[\beta]) C_{23} + \\ & \frac{1}{4} \delta(\omega + (\Omega - \Lambda)) ((1 + \cos[\beta]) \sin[\alpha] + (-1 + \cos[\alpha]) \sin[\beta]) C_{23} - \\ & \frac{1}{4} \delta(\omega - (\Omega - \Lambda)) ((-1 + \cos[\beta]) \sin[\alpha] + (1 + \cos[\alpha]) \sin[\beta]) C_{23} - \\ & \frac{1}{4} \delta(\omega - (\Omega + \Lambda)) ((1 + \cos[\beta]) \sin[\alpha] + (1 + \cos[\alpha]) \sin[\beta]) C_{23} \end{aligned} $	$ \begin{aligned} & \frac{1}{4} \delta(\omega + (\Omega + \Lambda)) ((-1 + \cos[\beta]) \sin[\alpha] + (-1 + \cos[\alpha]) \sin[\beta]) C_{13} - \\ & \frac{1}{4} \delta(\omega + (\Omega - \Lambda)) ((1 + \cos[\beta]) \sin[\alpha] + (-1 + \cos[\alpha]) \sin[\beta]) C_{13} - \\ & \frac{1}{4} \delta(\omega - (\Omega - \Lambda)) ((-1 + \cos[\beta]) \sin[\alpha] + (1 + \cos[\alpha]) \sin[\beta]) C_{13} + \\ & \frac{1}{4} \delta(\omega - (\Omega + \Lambda)) ((1 + \cos[\beta]) \sin[\alpha] + (1 + \cos[\alpha]) \sin[\beta]) C_{13} - \\ & \frac{1}{8} \delta(2\omega - (\Omega + \Lambda)) (-1 + \cos[\alpha]) (-1 + \cos[\beta]) (C_{11} - C_{22}) + \\ & \frac{1}{8} \delta(2\omega - (\Omega - \Lambda)) (1 + \cos[\alpha]) (-1 + \cos[\beta]) (C_{11} - C_{22}) + \\ & \frac{1}{8} \delta(2\omega + (\Omega - \Lambda)) (-1 + \cos[\alpha]) (1 + \cos[\beta]) (C_{11} - C_{22}) - \\ & \frac{1}{8} \delta(2\omega - (\Omega + \Lambda)) (1 + \cos[\alpha]) (1 + \cos[\beta]) (C_{11} - C_{22}) \end{aligned} $	$ \begin{aligned} & -\frac{1}{2} \delta(2\omega + \Omega_{\text{el}}) (-1 + \cos[\alpha]) \sin[\beta] C_{12} + \\ & \frac{1}{2} \delta(2\omega - \Omega_{\text{el}}) (1 + \cos[\alpha]) \sin[\beta] C_{12} + \\ & \frac{1}{2} \delta(\omega + \Omega_{\text{el}}) \\ & (\cos[\beta] - \cos[\alpha] \cos[\beta] + \sin[\alpha] \sin[\beta]) C_{23} \end{aligned} $
$ \begin{aligned} & \frac{1}{2} \delta(\omega + \Omega \Lambda) (\cos[\alpha] (-1 + \cos[\beta]) - \sin[\alpha] \sin[\beta]) C_{13} + \\ & \frac{1}{4} \delta(2\omega + \Lambda) (-1 + \cos[\beta]) \sin[\alpha] (C_{11} - C_{22}) + \\ & \frac{1}{4} \delta(2\omega - \Lambda) (1 + \cos[\beta]) \sin[\alpha] (C_{11} - C_{22}) \end{aligned} $	$ \begin{aligned} & -\frac{1}{2} \delta(2\omega + \Lambda) (-1 + \cos[\beta]) \sin[\alpha] C_{12} + \\ & \frac{1}{2} \delta(2\omega - \Lambda) (1 + \cos[\beta]) \sin[\alpha] C_{12} + \\ & \frac{1}{2} \delta(\omega + \Omega \Lambda) (\cos[\alpha] - \cos[\alpha] \cos[\beta] + \sin[\alpha] \sin[\beta]) C_{23} \end{aligned} $	$ \begin{aligned} & \frac{1}{2} (\sin[\alpha] \sin[\beta] C_{11} + \\ & \sin[\alpha] \sin[\beta] C_{22} + 2 \cos[\alpha] \cos[\beta] C_{33}) \end{aligned} $

Figure S9: Unlike spins : time average of the matrix $A_{\mu\nu}(ij)$. All time-averaged Hamiltonians for unlike spins presented in Section IVB of the main article follow from this expression.